Electronic Supplementary Material (ESI) for RSC Advances.

Electronic Supporting Information

Carbon molecular sieve membrane from a microporous spirobisindane-based polyimide precursor with enhanced ethylene/ethane mixed-gas selectivity

Octavio Salinas, Xiaohua Ma, Yingge Wang, Yu Han and Ingo Pinnau*

Advanced Membranes and Porous Materials Center, Physical Sciences and Engineering Division, King Abdullah University of Science and Technology (KAUST), Al-Jazri Building, Thuwal 23955-6900, Saudi Arabia.

Corresponding author E-mail: ingo.pinnau@kaust.edu.sa

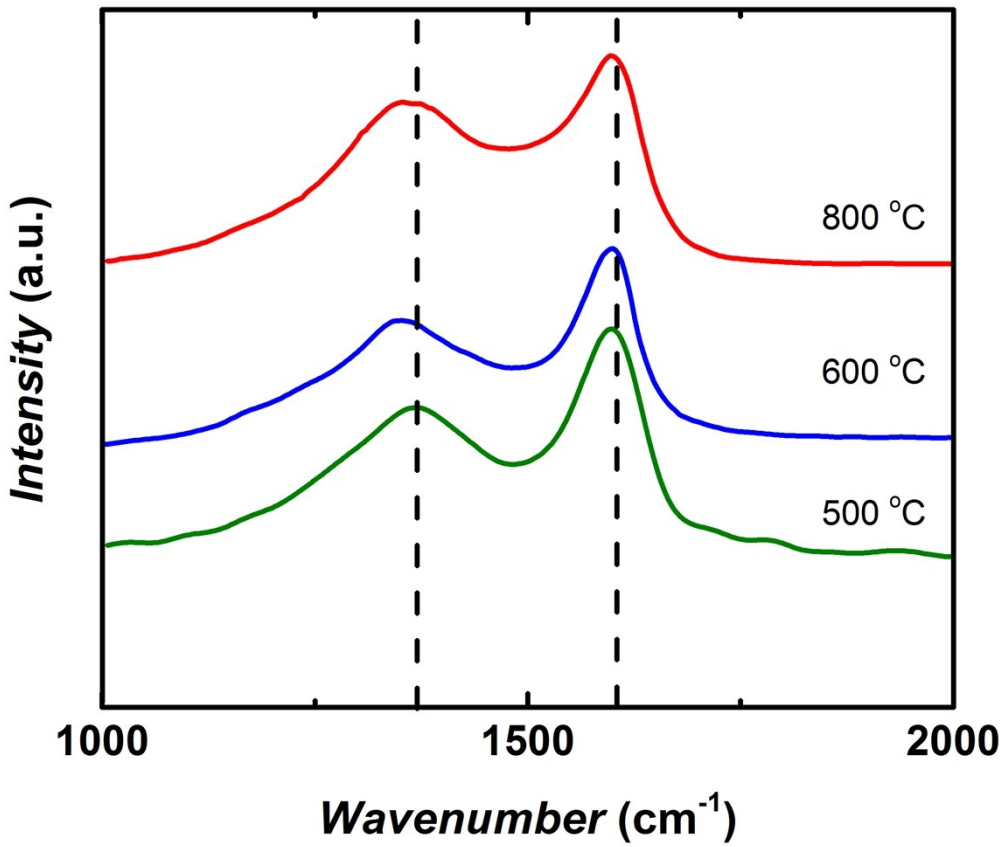

Fig. S1 Raman spectra of CMS generated from PIM-6FDA at 500, 600 and 800 °C. D and G peaks indicate the existence of amorphous graphite domains.

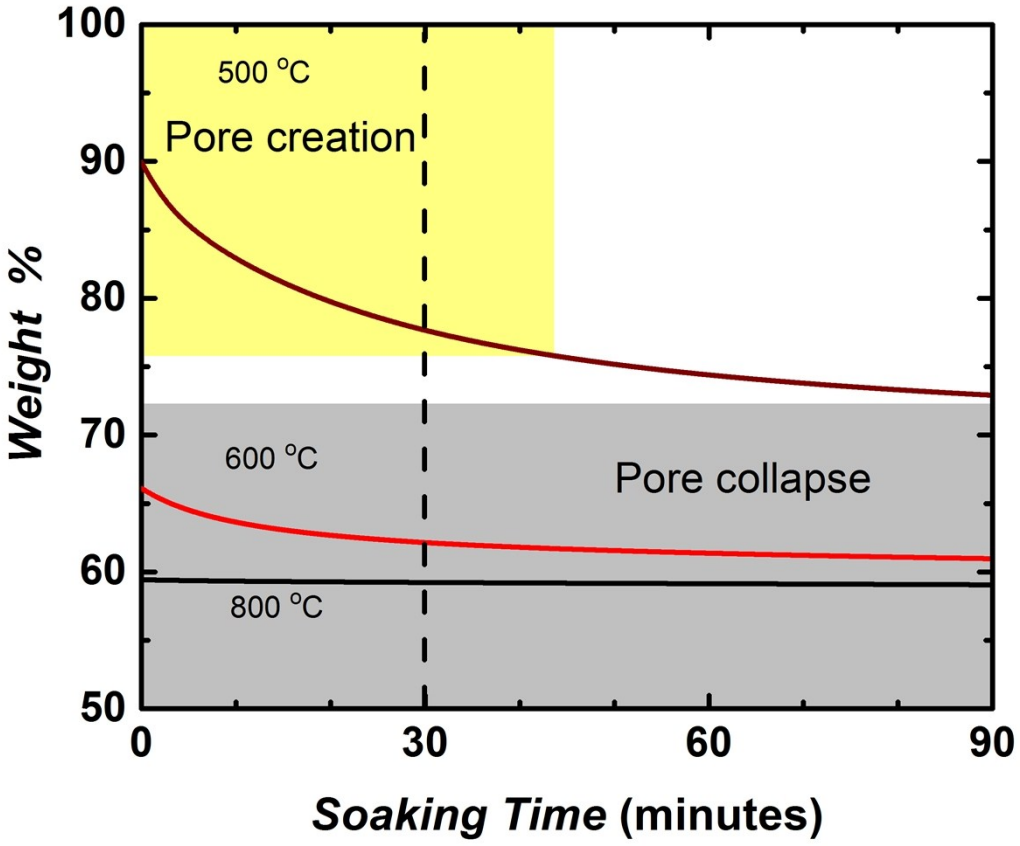

Fig. S2 Weight loss of PIM-6FDA for each isothermal stage of carbonization. Shaded areas show the dominating porosity evolution mechanisms during heat treatment while the dashed line was the actual soak time used in the pyrolysis protocol.

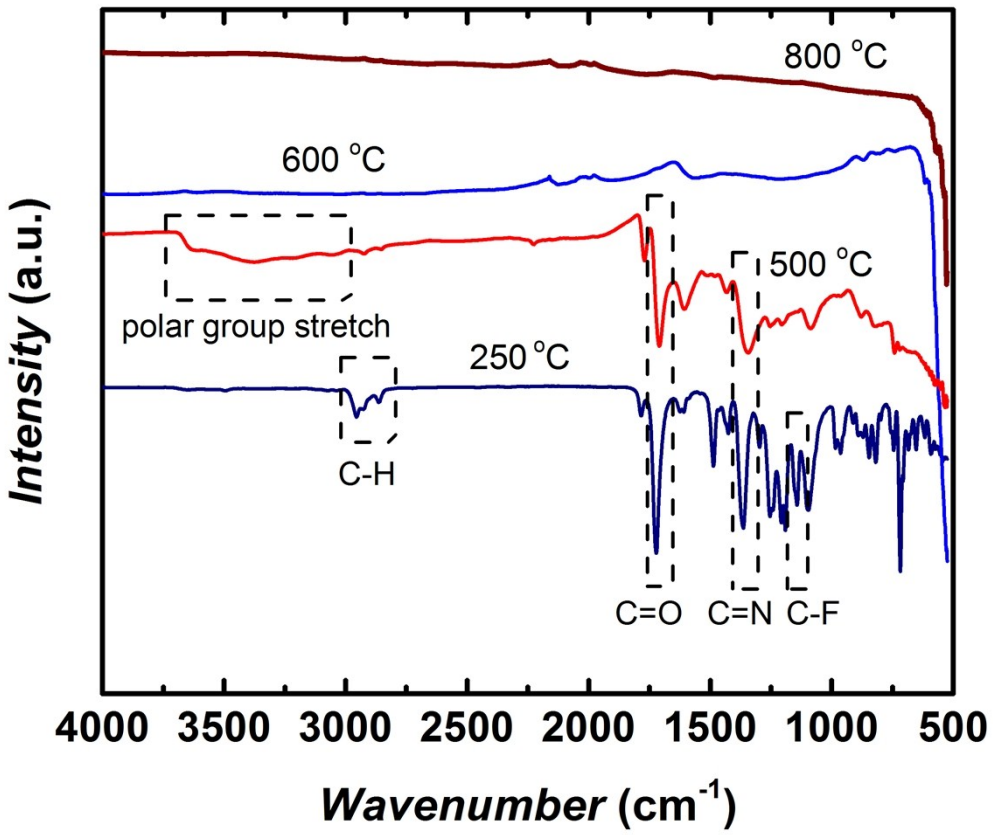

Fig. S3 FTIR spectra of PIM-6FDA and CMS membranes derived at 500, 600 and 800 **°**C.

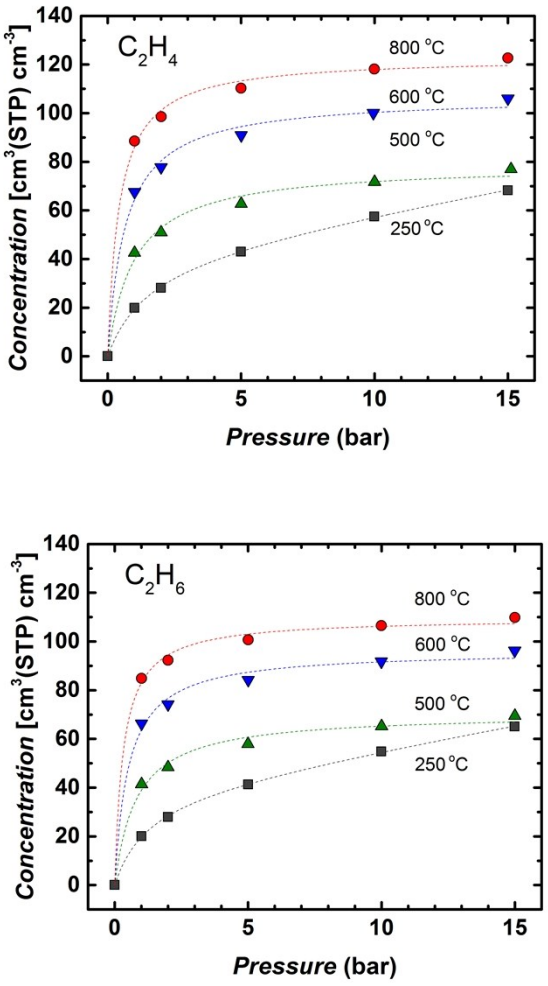

Fig. S4 Pure-gas sorption isotherms of C_2H_4 and C_2H_6 at 35 °C in PIM-6FDA and its CMS derivatives. Fitted dashed curves follow the dual-mode sorption model for the polymeric PIM-PI annealed at 250 °C, whereas the Langmuir model was used to describe sorption isotherms in the CMS samples.

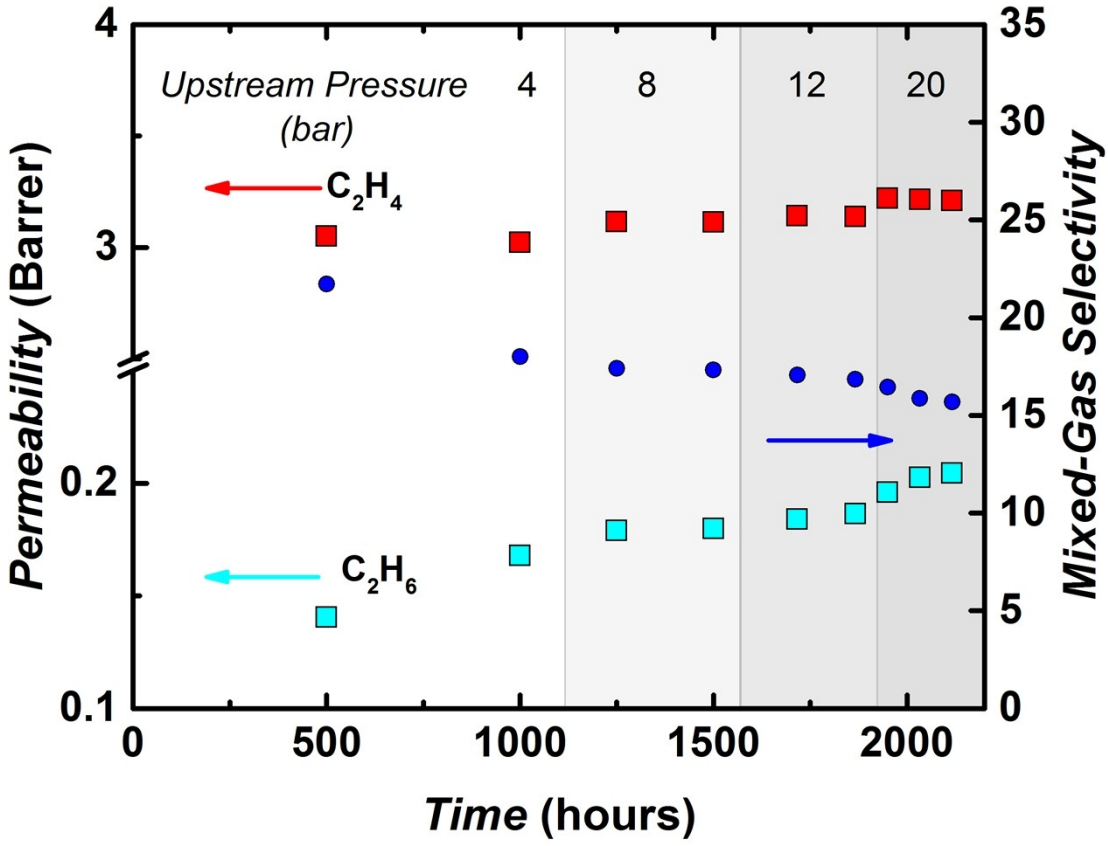

Fig. S5 Pressure- and time-dependence of the mixed-gas transport properties of a PIM-6FDA CMS membrane pyrolized at 800 °C (feed: 35 °C; 1:1 ethylene/ethane binary mixture).

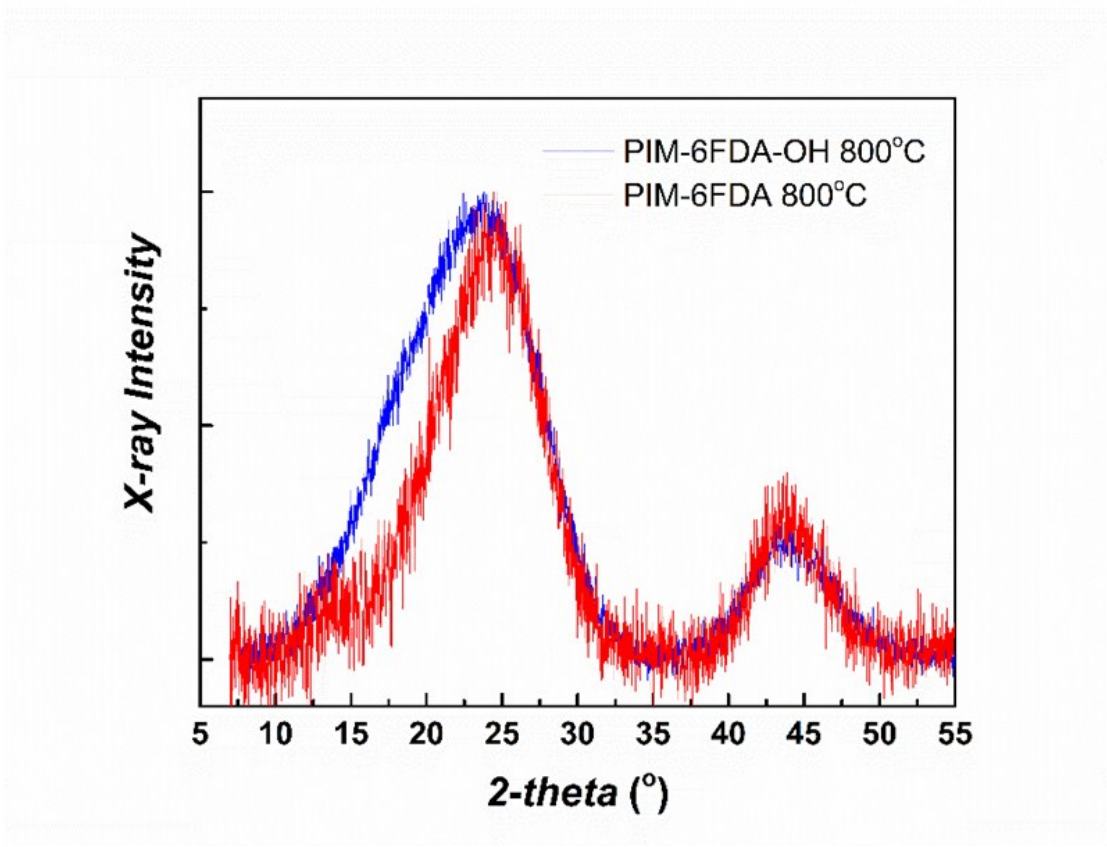

Fig. S6 Comparison of XRD spectra for PIM-6FDA-OH[1] (blue) and PIM-6FDA (red) CMS membranes pyrolized at 800 °C.

(a)

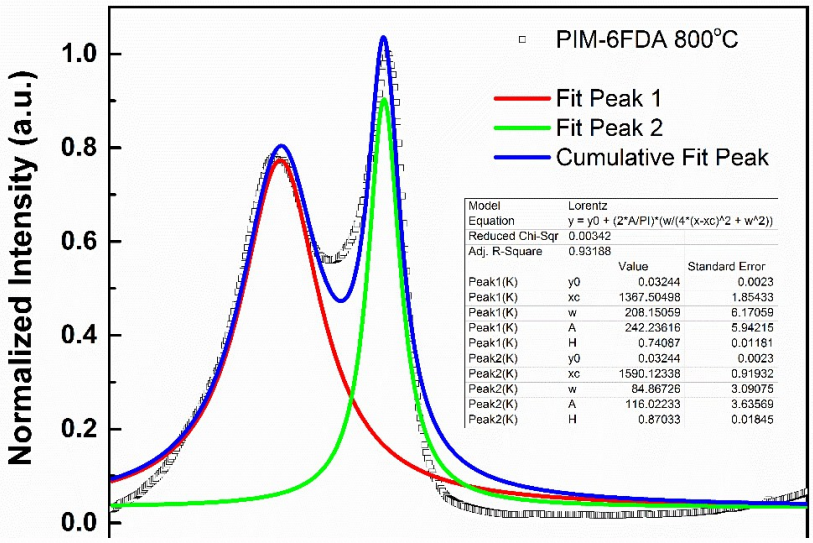

Model	Lorentz		
Equation	y = y0 + (2*A/PI)*(w/(4*(x-xc)^2 + w^2))		
Reduced Chi-Sqr	0.00342		
Adj. R-Square	0.93188		
		Value	Standard Error
Peak1(K)	y0	0.03244	0.0023
Peak1(K)	xc	1367.50498	1.85433
Peak1(K)	w	208.15059	6.17059
Peak1(K)	A	242.23616	5.94215
Peak1(K)	H	0.74087	0.01181
Peak2(K)	y0	0.03244	0.0023
Peak2(K)	xc	1590.12338	0.91932
Peak2(K)	w	84.86726	3.09075
Peak2(K)	A	116.02233	3.63569
Peak2(K)	H	0.87033	0.01845

(b)

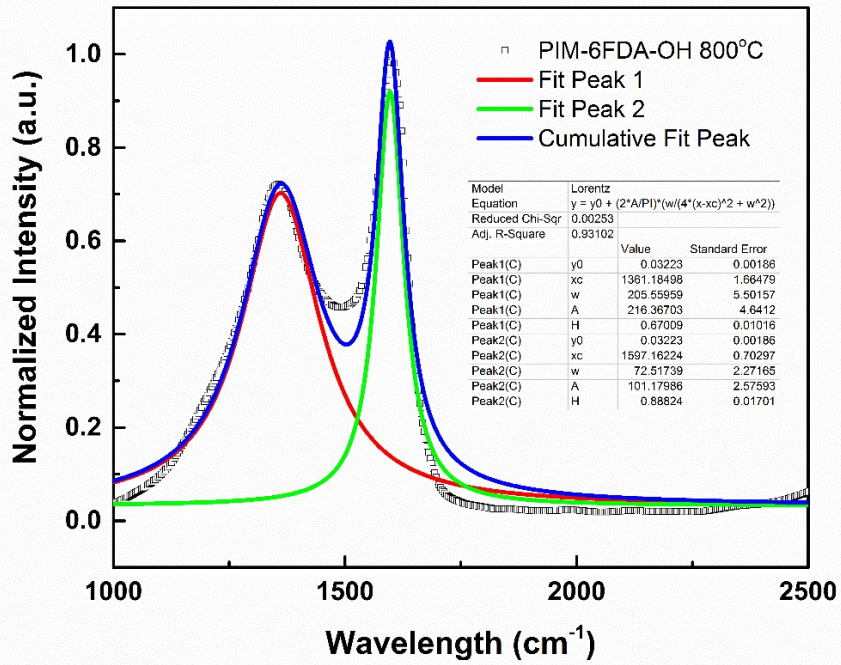

Model	Lorentz		
Equation	y = y0 + (2*A/PI)*(w/(4*(x-xc)^2 + w^2))		
Reduced Chi-Sqr	0.00253		
Adj. R-Square	0.93102		
		Value	Standard Error
Peak1(C)	y0	0.03223	0.00186
Peak1(C)	xc	1361.18498	1.66479
Peak1(C)	w	205.55959	5.50157
Peak1(C)	A	216.36703	4.6412
Peak1(C)	H	0.67009	0.01016
Peak2(C)	y0	0.03223	0.00186
Peak2(C)	xc	1597.16224	0.70297
Peak2(C)	w	72.51739	2.27165
Peak2(C)	A	101.17986	2.57593
Peak2(C)	H	0.88824	0.01701

Fig. S7 Raman spectra analysis with peak fitting for (a) PIM-6FDA CMS pyrolized at 800 °C and (b) PIM-6FDA-OH CMS[1] pyrolized at 800 °C.

Table S1. Gravimetric densities of PIM-6FDA, PIM-6FDA-OH and their CMS derivatives.

Treatment temperature (°C)	Bulk density (g/cm^3)	
	PIM-6FDA	PIM-6FDA-OH
250	1.24	1.28
400	1.24	1.18
500	1.21	1.20
600	1.31	1.32
800	1.53	1.50

[a]Measured gravimetrically, ρ=(weight of sample)/(volume)

Table S2 Parameters obtained from fitting experimental data to the dual-mode model for pristine PIM-6FDA and Langmuir isotherms for CMS membranes.[a]

Membrane type	C_2H_4			C_2H_6		
	K_d	C'_H	b	k_d	C'_H	b
PIM-6FDA 250 °C	2.57	43.5	0.9	2.54	39.7	1.1
CMS 500 °C		79.0	1.3		70.6	1.6
CMS 600 °C		106.9	2.0		96.3	2.6
CMS 800 °C		123.0	3.1		109.6	4.2

[a] K_d [10^{-2} cm^3(STP) cm^{-3} cmHg^{-1}]; C'_H [cm^3(STP) cm^{-3}]; b [10^{-2} cmHg^{-1}]

Table S3 Parameters obtained from fitting Raman spectra with excitation wavelength 473 nm for CMS membranes at 800 °C derived from PIM-6FDA and PIM-6FDA-OH.

Membrane type	I(D)/I(G)[a]	Pos (D)[b]	Pos (G)[c]
PIM-6FDA 800 °C CMS	2.08	1367.5	1590.1
PIM-6FDA-OH 800 °C CMS	2.14	1361.2	1597.2

a) Intensity ratio of D band vs. G band, calculated as the peak area ratio of D band and G band using Lorentz fitting from Fig. S7.[2] A lower I(D)/I(G) ratio is likely to be associated with lower defects density and higher order in graphitic materials. However, caution needs to be taken into account because such interpretation only works in the domain of graphitic like materials with small crystallite size. Based on XRD analysis, we estimated a crystallite size of around 4.2 nm. Such size is very close to the critical size, below which I(D)/I(G) ratio increases as a function of defect density, above which I(D)/I(G) ratio decrease as a function of defect density.[3] Therefore, conclusions based on Raman analysis have to be taken with some caution.

b) Position of D band in the Raman spectra from fitting.

c) Position of G band in the Raman spectra from fitting.

References:

1. O. Salinas, X. Ma, E. Litwiller and I. Pinnau, *J. Membr. Sci.*, 2016, **500**, 115-123.
2. C. Sisu, R. Iordanescu, V. Stanciu, I. Stefanescu, A.M. Vlaicu, and V.V. Grecu, *Dig. J. Nanomater. Bios.*, 2016, **11**, 435-442.
3. A. C. Ferrari and D.M. Basko, *Nat. Nanotechnol*, 2013, **8**, 235-246.